The Astrophysical Journal, 727:103 (7pp), 2011 February 1 doi:10.1088/0004-637X/727/2/103
© 2011. The American Astronomical Society. All rights reserved. Printed in the U.S.A.

THE ANGLO-AUSTRALIAN PLANET SEARCH. XX. A SOLITARY ICE-GIANT PLANET ORBITING HD 102365*

C. G. Tinney[1], R. Paul Butler[2], Hugh R. A. Jones[3], Robert A. Wittenmyer[1], Simon O'Toole[4], Jeremy Bailey[1], and Brad D. Carter[5]

[1] Department of Astrophysics, School of Physics, University of New South Wales, NSW 2052, Australia; c.tinney@unsw.edu.au
[2] Department of Terrestrial Magnetism, Carnegie Institution of Washington, 5241 Broad Branch Road NW, Washington, DC 20015-1305, USA
[3] Centre for Astrophysical Research, University of Hertfordshire, Hatfield, AL10 9AB, UK
[4] Australian Astronomical Observatory, P.O. Box 296, Epping, NSW 1710, Australia
[5] Faculty of Sciences, University of Southern Queensland, Toowoomba, Queensland 4350, Australia
Received 2010 October 12; accepted 2010 November 24; published 2011 January 10

ABSTRACT

We present 12 years of precision Doppler data for the very nearby G3 star HD 102365, which reveals the presence of a Neptune-like planet with a 16.0 $M_{\rm Earth}$ minimum mass in a 122.1 day orbit. Very few "Super Earth" planets have been discovered to date in orbits this large and those that have been found reside in multiple systems of between three and six planets. HD 102365 b, in contrast, appears to orbit its star in splendid isolation. Analysis of the residuals to our Keplerian fit for HD 102365 b indicates that there are no other planets with minimum mass above 0.3 $M_{\rm Jup}$ orbiting within 5 AU and no other "Super Earths" more massive than 10 $M_{\rm Earth}$ orbiting at periods shorter than 50 days. At periods of less than 20 days these limits drop to as low as 6 $M_{\rm Earth}$. There are now 32 exoplanets known with minimum mass below 20 $M_{\rm Earth}$, and interestingly the period distributions of these low-mass planets seem to be similar whether they orbit M-, K-, or G-type dwarfs.

Key words: planetary systems – stars: individual (HD 102365)

Online-only material: color figure

1. INTRODUCTION

In recent years, extending the threshold for exoplanet detection to yet lower and lower masses has been a significant endeavor for exoplanetary science. As at 2010 October, 31 exoplanets have been published with minimum (i.e., $m \sin i$) masses of less than 20 $M_{\rm Earth}$. All have been found in orbits of less than a few hundred days, corresponding to orbital radii of $\lesssim$1 AU. Roughly equal numbers have been found orbiting M-, K-, and G-type dwarfs (10, 11, and 10, respectively, in each of these spectral types). This roughly equal distribution hides several selection effects. First, that finding very low-mass planets orbiting G-dwarfs is *much* harder than finding them orbiting M-dwarfs, since the lower mass of an M-dwarf primary will (for a given mass planet with a given orbital period) make the Doppler amplitude of an M-dwarf exoplanet at least three times larger than a G-dwarf one. And second, that current planet search target lists are dominated by G-dwarfs.

The detection of such low-mass exoplanets has in large part been due to the dramatic improvements achieved in the intrinsic, internal measurement precisions of Doppler planet search facilities. These have improved to such an extent that noise sources *intrinsic* to the parent star are the major limiting factor for very low-mass exoplanet detection. Characterization of these noise sources (jitter, convective granulation, and asteroseismological p-mode oscillations) has become an important focus of Doppler planet detection. A few obvious modifications to current observing strategies have emerged—(1) target low-mass stars; (2) target chromospherically inactive and slowly rotating stars; (3) target high-gravity stars (where p-mode oscillations are minimized); and (4) extend the observations of stars over several p-mode fundamental periods, so that asteroseismological noise is suppressed.

The Anglo-Australian Planet Search (AAPS) began operation in 1998 January and is currently surveying 250 stars. It has first discovered 33 exoplanets with $m \sin i$ ranging from 5.1 $M_{\rm Earth}$ to 10 $M_{\rm Jup}$ (Tinney et al. 2001, 2002, 2003, 2005, 2006; Butler et al. 2001, 2002; Jones et al. 2002, 2003a, 2003b, 2006, 2010; Carter et al. 2003; McCarthy et al. 2004; O'Toole et al. 2007, 2009; Bailey et al. 2009; Vogt et al. 2010b). Over the last five years, each of the observing strategy improvements listed above have been implemented in this planet search program, resulting in the detection of several low-amplitude systems in recent years (e.g., 61 Vir bcd, HD 16417b—Vogt et al. 2010b; O'Toole et al. 2009). In this paper, we add to this track record, with the discovery of a 16 $M_{\rm Earth}$ planet in a 122.1 $\pm$ 0.3 day orbit around the very nearby (d = 9.24 pc) G3 star HD 102365.

2. HD 102365

HD 102365 (Gl 442A, HIP 57443, and LHS 311) lies at a distance of 9.24 $\pm$ 0.06 pc (Perryman et al. 1997) and has been classified as both a G3V (Keenan & McNeil 1989) and a G5V (Evans et al. 1957). It has an absolute magnitude of $M_{\rm V}$ = 5.06 (V = 4.89) and $B - V$ = 0.664. *Hipparcos* photometry finds it to be photometrically stable at the 4 mmag level over 112 observations over the course of the *Hipparcos* mission (Perryman et al. 1997).

HD 102365 was identified by Van Biesbrock (1961) as being a member of a common-proper-motion binary system. Its companion star (LHS 313, Gl 442B) is considerably fainter (V = 15.43). Hawley et al. (1996) identified the companion as an M4V, and it was recovered by Two Micron All Sky Survey at a position angle and separation consistent with the earlier

* Based on observations obtained at the Anglo-Australian Telescope, Siding Spring, Australia.

Table 1
Properties of HD 102365

Reference	$T_{\rm eff}$	[Fe/H]	Mass	log(g)	Age	$v \sin i$	$R'_{\rm HK}$
Valenti & Fischer (2005) and Takeda et al. (2007)[a]	5630 K	−0.26	$0.89 \pm 0.03\ M_{\odot}$	4.57	9 ± 3 Gyr[l]	0.7 km s^{-1}	...
Sousa et al. (2008)	5629 ± 29 K[b]	-0.29 ± 0.02	$0.82\ M_{\odot}$	4.44 ± 0.02	...	...	...
Holmberg et al. (2009)	5650 K	−0.33	...	...	...	...	...
Gray et al. (2006)	5688 K	−0.33	...	4.51	...	...	...
Bond et al. (2006)	5688 ± 100 K	-0.28 ± 0.07	...	4.7 ± 0.2	...	...	...
Schröder et al. (2009)	...	...	...	...	...	...	−5.03
Henry et al. (1996)	...	...	...	...	...	...	−4.95

Notes.
[a] Mass and age from Takeda et al. (2007), remaining parameters from Valenti & Fischer (2005).
[b] $T_{\rm eff}$ from infrared flux method.

identification, and had optical-near-infrared colors consistent with being a binary companion to HD 102365. Its near-infrared photometry ($M_J = 8.8 \pm 0.2$) indicates a mass of 0.2 $M_{\odot}$ (using the mass–luminosity relations of Delfosse et al. 2000). The separation of the components on the sky corresponds to a distance of 322 AU, which would place the orbital period of the companion in the region of tens of thousands of years.

HD 102365 is a bright, nearby and Sun-like star. It has therefore been the subject of multiple atmospheric and isochronal analyses—the conclusions reached by the most recent of these are summarized in Table 1. In brief, HD 102365 is ≈100 K cooler than the Sun has a metallicity a factor of two lower (i.e., −0.3 dex) and a mass about 15% lower. In the analysis which follows we assume a mass of 0.85 $M_{\odot}$.

HD 102365 is also a very slow rotator ($v \sin i = 0.7$ km s^{-1}) and inactive (with a mean $R'_{\rm HK}$ from the two published measurements of −4.99). Its predicted stellar jitter due to activity is 2.1 m s^{-1} (using the updated Ca II jitter calibration of J. Wright 2008, private communication). Asteroseismology will also contribute jitter to observations of HD 102365, however this impact will be small at less than a 0.14 m s^{-1} rms noise equivalent (for observations of more than 10 minutes) using the relations of O'Toole et al. (2008).

3. OBSERVATIONS

AAPS Doppler measurements are made with the UCLES echelle spectrograph (Diego et al. 1990). An iodine absorption cell provides wavelength calibration from 5000 to 6200 Å. The spectrograph point-spread function and wavelength calibration are derived from the iodine absorption lines embedded on every pixel of the spectrum by the cell (Valenti et al. 1995; Butler et al. 1996).

Observations of HD 102365 began as part of the AAPS main program in 1998 January, and over the following seven years it was observed regularly in observations of 200–400 s (depending on observing conditions) giving a signal-to-noise ratio (S/N) of ≈200 per spectral pixel in the iodine region. These are the observations listed in Table 2 between JD = 2450830.212–2453402.195. In 2005 April, HD 102365 (together with a number of other bright AAPS targets) was elevated within our observing program to high-S/N status, such that its target S/N per epoch became 400 per spectral pixel. As a result the median internal uncertainties produced by our Doppler fitting process dropped from 1.55 m s^{-1} to 0.89 m s^{-1}. The Doppler velocities derived from all these observations are listed in Table 2.

4. ANALYSIS

The root-mean-square (rms) scatter about the mean velocity of all AAPS data for HD 102365 is 3.0 m s^{-1}, which is higher by ≈1 m s^{-1} than would be expected based on measurement precision and stellar jitter alone.

Figure 1 shows a Two-Dimensional Keplerian Lomb–Scargle periodogram (2DKLS; O'Toole et al. 2007) of these data. The 2DKLS extends the concept of the traditional Lomb–Scargle (LS) periodogram by fitting Keplerians to the data as a function of period and eccentricity and allows the identification of an indicated eccentricity (e) as well as an indicated period (P) from a time series of Doppler velocities. The HD 102365 data display an extremely strong peak at a period of 122 days in the two-dimensional 2DKLS plane (Figure 1 upper panel) with the period peak showing no strong dependence on eccentricity, but with a detectable maximum at $e = 0.36$. The power spectrum is shown as a one-dimensional spectrum at $e = 0.36$ in the lower panel of Figure 1.

Figure 2 (upper panel) shows a traditional LS periodogram (Lomb 1976; Scargle 1982) for this data set, along with estimated false alarm probability limits overlain at 0.1%, 1%, and 10% as generated by the Systemic Console code (Meschiari et al. 2009). The 122 day peak appears at a timescale considerably longer than would be expected if it were associated with the rotation period of this star, which even though a slow rotator ($v \sin i = 0.7$ m s^{-1}) is nonetheless predicted to have a rotation period of ∼40 day on the basis of its low chromospheric activity (Noyes et al. 1984).

A least-squares Keplerian fit to the data using the 2DKLS peak as an initial estimate results in the orbital parameters shown in Table 3. Figure 3 displays this fit (and the residuals to it) as a function of orbital phase. The rms scatter to this fit is 2.53 m s^{-1}, and the reduced chi-squared (χ^2_{ν}) is 1.078. This fit indicates the presence of a planet with period 122.1 ± 0.3 day, eccentricity 0.34 ± 0.14, semimajor axis 0.46 ± 0.04 AU, and minimum mass ($m \sin i$) 16.0 ± 2.6 $M_{\rm Earth}$. Eccentricities in such Doppler fits are usually quite poorly constrained, and the covariance matrix-based uncertainties quoted in Table 3 typically overestimate their actual precision. Indeed, a bootstrap-based uncertainty estimate for e in this solution Meschiari et al. (2009) indicates the 90% confidence interval on e is ±0.34—consistent with zero eccentricity. We therefore also quote in the table an orbital solution for a fixed eccentricity of $e = 0.0$. This solution is marginally poorer than the solution with e allowed to float ($\chi^2_{\nu} = 1.098$, rms = 2.57), but results in the same semimajor axis and minimum-mass estimates being derived for the planet.

Table 2
Velocities for HD 102365

JD (−2450000)	RV (m s^{-1})	Uncertainty (m s^{-1})	JD (−2450000)	RV (m s^{-1})	Uncertainty (m s^{-1})	JD (−2450000)	RV (m s^{-1})	Uncertainty (m s^{-1})
830.2120	−1.95	1.46	3517.8765	+2.14	0.85	4146.1494	+1.52	0.66
970.8882	+0.45	1.20	3518.9348	+2.26	0.78	4147.1817	−0.86	0.66
1213.2263	−7.71	1.44	3519.8345	+2.54	0.91	4148.2115	−0.21	0.78
1237.1088	−4.49	2.15	3520.9700	+2.15	0.94	4149.1503	−1.44	0.76
1274.1669	−1.60	1.25	3521.9180	+0.27	0.95	4150.1458	−0.86	0.70
1275.0686	−10.58	2.16	3522.9518	+1.36	0.87	4151.1931	−1.09	0.73
1382.9017	−6.39	1.40	3568.8441	−2.98	0.84	4152.2082	+1.83	0.89
1631.0427	−5.16	1.45	3569.8610	−0.63	0.93	4153.1592	−2.80	0.86
1682.8377	−4.44	1.65	3570.8839	−2.77	0.90	4154.1097	−2.22	0.60
1684.0503	+1.24	1.53	3571.8931	−3.66	0.89	4155.0789	−0.69	0.72
1717.8540	−3.41	1.48	3572.8653	−1.53	0.87	4156.0537	−2.32	1.09
1743.8680	−1.76	1.47	3573.8496	−4.95	0.85	4222.0454	−0.22	1.65
1919.2349	+0.45	2.40	3575.8540	−2.77	0.82	4223.0693	+1.29	0.97
1984.1277	−6.26	1.77	3576.8510	−1.98	0.79	4224.0894	+1.72	0.94
2009.1581	+0.22	1.39	3577.8470	−2.68	0.84	4225.0363	−1.85	0.82
2060.9266	−1.34	1.51	3578.8456	−2.01	0.85	4226.0030	−1.80	1.28
2127.8671	−3.53	1.99	3700.2461	+0.96	0.94	4252.9565	−1.44	0.93
2388.0430	−6.22	1.48	3753.2481	+0.78	1.09	4254.9066	+1.08	1.00
2420.9725	−0.04	1.55	3840.1183	−7.07	1.24	4255.9285	−2.85	1.01
2421.9764	+1.17	1.45	3841.0030	−1.04	0.84	4257.0523	−3.52	1.08
2422.9051	−0.06	1.57	3844.0169	+0.14	0.87	4543.1122	−4.10	0.75
2423.9770	+1.28	1.82	3937.8743	−0.07	0.82	4550.0793	+0.13	1.36
2424.9796	−0.47	1.11	4038.2472	−2.10	1.27	4551.0414	−2.21	1.00
2455.8883	−7.60	1.53	4111.1843	+3.31	0.85	4553.0691	−3.15	1.12
2654.2716	+2.56	1.63	4112.1940	+2.14	0.74	4841.2280	+3.19	1.08
2745.0216	−2.85	1.57	4113.2161	+3.27	0.88	4843.2598	+0.42	1.12
2749.0801	−2.38	1.61	4114.2235	+1.65	0.85	4897.1422	−0.24	0.99
2751.0742	+1.54	1.66	4115.2295	+0.53	1.09	4901.1335	−5.34	1.14
2783.9628	+1.35	1.67	4119.2316	+1.64	0.82	4902.1479	−2.55	1.12
2860.8442	+3.75	1.62	4120.1772	−0.70	0.69	4904.1774	−5.32	1.44
3005.2531	+6.60	2.02	4121.1826	−0.72	0.67	4905.1780	−4.82	0.94
3008.2151	+1.99	1.58	4123.2074	+2.98	0.64	4906.1968	−1.83	1.08
3041.2850	+5.84	1.47	4126.1448	−1.41	0.69	4908.1785	−2.15	0.95
3042.2136	+0.61	1.52	4127.1543	+3.39	0.62	5031.8906	−4.38	0.90
3048.2584	+0.72	1.63	4128.1690	+0.93	0.85	5202.1955	+5.43	1.20
3051.1885	+4.38	1.45	4129.1708	−1.06	0.60	5204.2366	+1.89	1.35
3214.8709	−0.20	1.55	4130.1644	+3.29	0.65	5206.1761	+1.41	1.00
3245.8512	−0.60	2.21	4131.1706	+2.19	0.70	5231.1466	+3.39	1.08
3402.1950	+0.58	0.82	4132.1780	+0.83	0.92	5253.1614	+3.46	0.97
3482.9418	+1.74	0.93	4133.2403	+2.29	0.97	5310.0451	−3.80	1.19
3483.9734	−2.73	0.87	4134.2021	+1.00	1.00	5312.0515	−2.28	1.03
3485.0087	−0.47	0.75	4135.1689	+2.68	0.85	5313.0652	+4.32	1.12
3485.9286	−2.12	0.93	4136.1870	+2.37	0.79	5314.9743	−2.40	0.97
3486.9909	−1.12	0.78	4137.1852	+3.04	0.65	5316.9911	−1.10	1.11
3488.0592	−2.55	0.78	4138.1656	+0.92	1.09	5370.8847	−0.66	1.20
3488.9752	−1.02	0.77	4139.1564	+2.89	0.82	5371.8836	−6.70	1.02
3506.9189	+0.23	0.87	4140.1589	+3.69	0.93	5374.9315	+5.32	1.47
3509.0173	+0.99	0.86	4141.1830	+4.62	0.89	...	...	...
3509.8462	−1.94	0.83	4142.1777	+3.48	0.60	...	...	...
3515.8545	+2.60	0.81	4144.0637	+2.47	0.73	...	...	...
3516.8477	+3.16	0.87	4145.1442	+3.08	0.75	...	...	...

To test the probability that the noise in our data might have resulted in a false detection, we have run simulations using the "scrambled velocity" approach of Marcy et al. (2005). This technique makes the null hypothesis that no planet is present and then uses the actual data as the best available proxy for the combined noise due to our observing system and the star. Multiple realizations are created by scrambling the observed velocities amongst the observed epochs. We created 5000 of these scrambled velocity sets, and then subjected them to the same analysis as our actual data set (i.e., identifying the strongest peak in the 2DKLS followed by a least-squares Keplerian fit). No trial amongst 5000 showed a χ^2_ν better than that obtained for the original data set, and the distribution of the scrambled reduced χ^2_ν (see Figure 4) shows a clear separation from that obtained with the actual data. We conclude that there is a less than 0.02% probability of us having obtained a false detection due to a fortuitous selection from a system with no planet.

Figure 2 (lower panel) shows the power spectrum of the residuals to the AAPS velocities with the fitted Keplerian removed, along with recalculated false alarm probabilities at

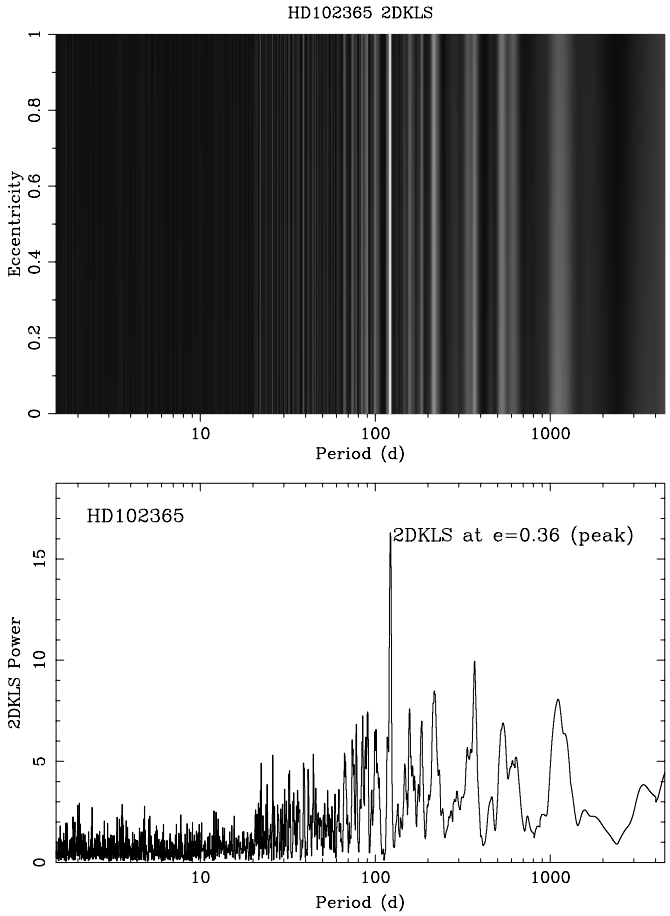

Figure 1. 2DKLS periodograms for HD 102365. The upper panel shows the periodic power as a function of assumed planet eccentricity and period. The lower panel shows a cut through the 2DKLS at $e = 0.36$ (the location of the peak power in the upper panel).

Table 3
Orbital Solution for HD 102365 b

Parameter	Eccentric Fit	Circular Fit
Orbital period P (days)	122.1 ± 0.3	122.2 ± 0.3
Velocity semiamplitude K (m s^{-1})	2.40 ± 0.35	2.27 ± 0.35
ω (deg)	105 ± 22	13 ± 35
Eccentricity e	0.34 ± 0.14	(0.0)
Periastron date (JD−2450000)	129 ± 11	93 ± 12
$m \sin i$ ($M_{\rm Earth}$)	16.0 ± 2.6	16.0 ± 2.6
Semimajor axis (AU)	0.46 ± 0.04	0.46 ± 0.04
$N_{\rm fit}$	149	149
rms (m s^{-1})	2.53	2.57

10%, 1%, and 0.1%. No other significant periodicities are present in the data once the 122 day planetary signal is removed.

5. DISCUSSION

The planet HD 102365 b has a Neptune-like minimum mass ($m \sin i = 16.0 \pm 2.6\ M_{\rm Earth}$) and moves in an orbit equivalent to the Mercury–Venus region of the inner solar system, with a periastron of 0.30 AU (cf. Mercury orbits from 0.307 AU to 0.466 AU) and an apastron of 0.61 AU (Venus orbits from 0.718 AU to 0.728 AU). This places it in a very small group of sub-20 $M_{\rm Earth}$ planets to have been detected at orbital periods beyond that of Mercury—just three such planets have been

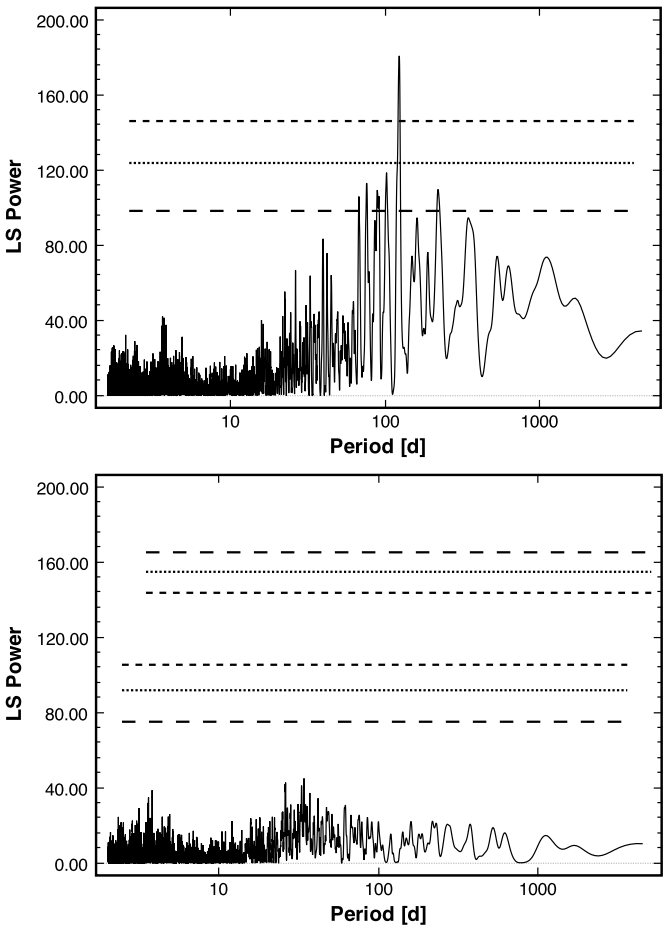

Figure 2. Traditional LS periodograms for HD 102365. Upper panel: with the false alarm probability levels of 10%, 1%, and 0.1%. Lower panel: the same data with the fitted planet removed and the false alarm probability levels of 10%, 1%, and 0.1% recalculated. No significant signal is detectable due to a further planet.

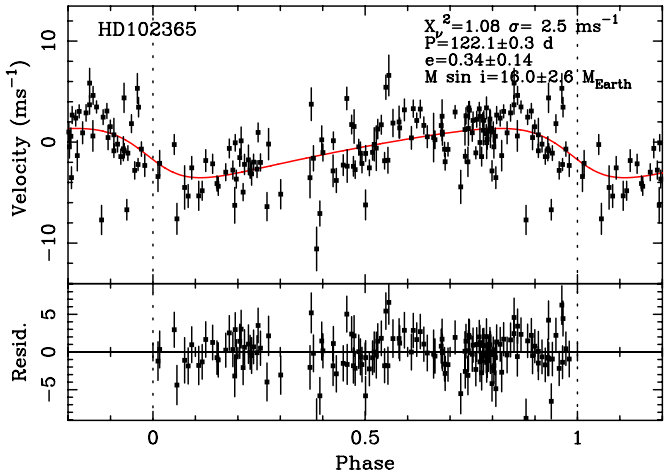

Figure 3. Keplerian best fit to Doppler data for HD 102365 phased at the best-fit period. The lower panel shows the residuals to the fit. A host star mass of 0.85 $M_\odot$ and an intrinsic stellar Doppler variability (i.e., jitter) of 2.1 m s^{-1} are assumed.

(A color version of this figure is available in the online journal.)

detected by precision Doppler planet searches to date. They are Gl 876e ($m \sin i = 14.6\ M_{\rm Earth}$, $P = 124.3$ day, primary is M4 with 0.32 $M_\odot$; Laughlin et al. 2005); HD 69830d ($m \sin i = 18\ M_{\rm Earth}$, $P = 197$ day, primary is K0 with 0.86 $M_\odot$; Lovis et al.

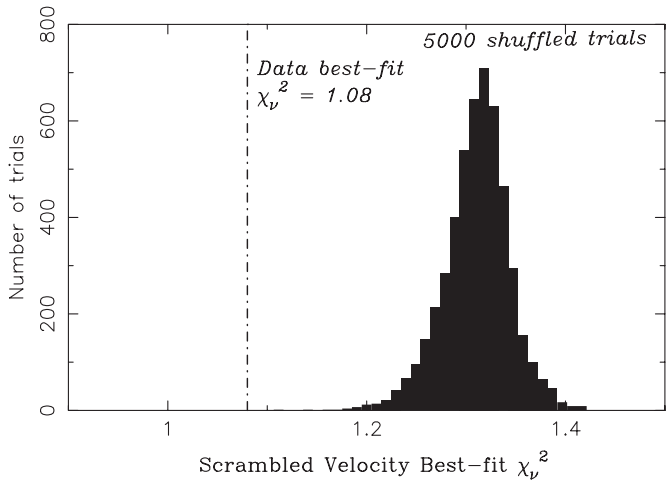

Figure 4. Scrambled false alarm probability results. The histogram shows the χ^2_ν values that result from the best Keplerian fits to 5000 realizations of scrambled versions of the AAPS velocities for HD 102365. The dashed line shows the reduced χ^2_ν for our actual data.

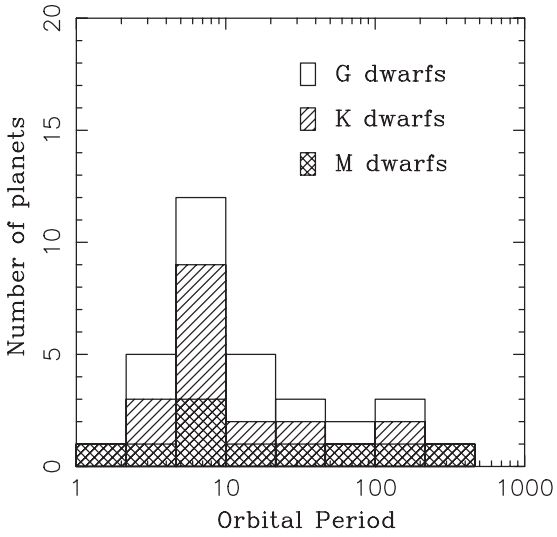

Figure 5. Period distribution for the 32 exoplanets currently known with minimum mass $m \sin i < 20\ M_{\rm Earth}$ (including HD 102365 b).

2004); and Gl 581f ($m \sin i = 7.0\ M_{\rm Earth}$, $P = 433$ day, primary is M3 with 0.31 $M_\odot$; Bonfils et al. 2005; Vogt et al. 2010a). Two of these planets orbit much lower-mass M-dwarfs (Gl 876e & Gl 581f), while HD 69830 orbits a K0 dwarf estimated to have a similar mass to that of HD 102365.

Table 4 lists the 32 radial velocity exoplanets currently known with minimum masses less than 20 $M_{\rm Earth}$ (including HD 102365 b) and Figure 5 shows their period distribution. There is a noticeable "pile-up" of such planets at periods of just less than 10 days, which is primarily an understandable result of two selection effects. First, since Doppler amplitude is a strong function of orbital period, planets of a given mass will be more readily detectable at short periods, than at long periods. And second, detecting a planet at a very short period (i.e., less than 2 days) is very hard in typical Doppler survey data sets, due to the strong aliasing imposed by the diurnal observing pattern. These two effects conspire to produce a peak in exoplanet detectability at 4–10 days for very low mass exoplanets.

What *is* interesting to note is that the period distribution is very similar for M-, K-, and G-type dwarf primaries. Given that

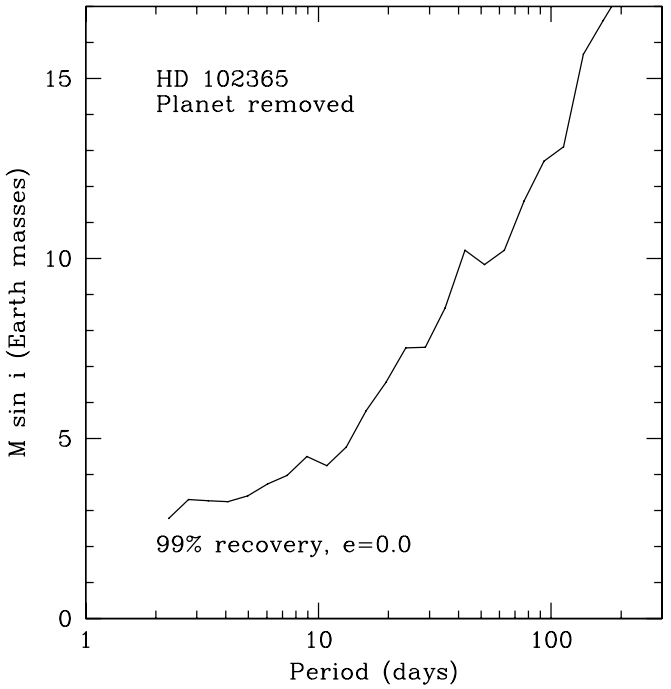

Figure 6. Detection limits (at 99% confidence level) for the presence of additional planets in the residuals to our one-planet fit for HD 102365 b.

these correspond to a variation in typical primary mass of a factor of three (and also presumably of the mass of the protoplanetary disk from which these planets formed), this would suggest that the process of forming sub-Neptune mass planets—and then migrating them in to radii of less than 0.6 AU—is not a strong function of stellar or disk mass.

The three planets noted above with similar properties to HD 102365 b (Gl 876e, HD 69830d, and Gl 581f) *all* lie in multiple systems. The HD 69830 system is a triple, while the two M-dwarfs (Gl 876 and Gl 581) host four and six exoplanets, respectively. In contrast, our HD 102365 data show no evidence for additional planets (see Figure 2). We computed the detectability of additional planets in the residuals to our one-planet fit, using the method of Wittenmyer et al. (2006, 2010). In brief, we add a Keplerian signal to the existing velocity data, then attempt to recover that signal using an LS periodogram. The mass of the simulated planet is increased until 99% of the injected signals are recovered with FAP $< 0.1\%$. The results of this analysis are shown for $P < 300$ days in Figure 6. Averaged over periods of less than 400 days (corresponding to $a < 1$ AU), our data exclude the presence of planets in circular orbits down to a Doppler amplitude of $K = 1.8 \pm 0.4$ m s^{-1}; that is, there are no "Super Earth" exoplanets more massive than 10 $M_{\rm Earth}$ orbiting at periods of less than 50 days in the HD 102365 system, and no planets more massive than 20 $M_{\rm Earth}$ within 1 AU. Furthermore, our data rule out all planets with $m \sin i > 0.3\ M_{\rm Jup}$ within 5 AU (corresponding to the 12.4 year duration of these observations). The HD 102365 system really does appear to contain just one ice-giant planet. It would be tempting to attribute the paucity of additional planets in this system to HD 102365's low metallicity of [Fe/H] $= -0.30$, and a resultant paucity of refractory elements for the formation of cores onto which planetary accretion can take place (Laughlin et al. 2004; Ida & Lin 2004, 2005), were it not for the similarly lower than solar metallicity of Gl 581 (though it must be acknowledged the determining metallicities for M-dwarfs is currently problematic,

Table 4
Exoplanets with Minimum Mass Below 20 $M_{\rm Earth}$

Planet	Mass ($M_{\rm Earth}$)	SpT	Period (day)	Orbit Ref.	Discovery Ref.
Gl 581 e	1.9	M3	3.14	Vogt et al. (2010a)	Mayor et al. (2009b)
Gl 581 g	3.1	M3	36.65	Vogt et al. (2010a)	Vogt et al. (2010a)
HD 156668 b	4.1	K3	4.64	Howard et al. (2010)	Howard et al. (2010)
HD 40307 b	4.2	K2.5	4.31	Mayor et al. (2009a)	Mayor et al. (2009a)
61 Vir b	5.0	G5	4.21	Vogt et al. (2010b)	Vogt et al. (2010b)
Gl 581 c	5.6	M3	12.92	Vogt et al. (2010a)	Udry et al. (2007)
HD 215497 b	6.6	K3	3.93	Lo Curto et al. (2010)	Lo Curto et al. (2010)
Gl 876 d	6.8	M4	1.94	Rivera et al. (2010)	Rivera et al. (2005)
HD 40307 c	6.9	K2.5	9.62	Mayor et al. (2009a)	Mayor et al. (2009a)
Gl 581 d	5.6	M3	66.9	Vogt et al. (2010a)	Udry et al. (2007)
Gl 581 f	7.0	M3	433	Vogt et al. (2010a)	Vogt et al. (2010a)
HD 181433 b	7.5	K3	9.37	Bouchy et al. (2009)	Bouchy et al. (2009)
HD 1461 b	7.4	G0	5.77	Rivera et al. (2010)	Rivera et al. (2010)
55 Cnc e	8.0	G8	2.80	Fischer et al. (2008)	McArthur et al. (2004)
Gl 176 b	8.4	M2.5	8.78	Forveille et al. (2009)	Forveille et al. (2009)
HD 40307 d	9.2	K2.5	20.46	Mayor et al. (2009a)	Mayor et al. (2009a)
HD 7924 b	9.3	K0	5.40	Howard et al. (2009)	Howard et al. (2009)
HD 69830 b	10.2	K0	8.67	Lovis et al. (2006)	Lovis et al. (2006)
μ Ara d[a]	10.5	G3	9.63	Pepe et al. (2007)	Santos et al. (2004)
HD 10180 d	11.9	G1	16.36	Lovis et al. (2010)	Lovis et al. (2010)
GJ 674 b	11.1	M2.5	4.69	Bonfils et al. (2007)	Bonfils et al. (2007)
HD 69830 c	11.8	K0	31.6	Lovis et al. (2006)	Lovis et al. (2006)
HD 4308 b	12.8	G5	15.56	Udry et al. (2006)	Udry et al. (2006)
HD 10180 c	13.2	G1	5.76	Lovis et al. (2010)	Lovis et al. (2010)
BD-08 2823 b	14.4	K3	5.60	Hébrard et al. (2010)	Hébrard et al. (2010)
Gl 876 e	14.6	M4	124.3	Rivera et al. (2010)	Rivera et al. (2010)
Gl 581 b	15.6	M3	5.36	Vogt et al. (2010a)	Bonfils et al. (2005)
HD 102365 b	16.0	G3	122	This paper	This paper
HD 90156 b	18.0	G5	49.77	Mordasini et al. (2010)	Mordasini et al. (2010)
HD 190360 c	18.1	G6	17.11	Wright et al. (2009)	Vogt et al. (2005)
HD 69830 d	18.1	K0V	197	Lovis et al. (2006)	Lovis et al. (2006)
61 Vir c	18.2	G5	38.02	Vogt et al. (2010b)	Vogt et al. (2010b)

Note. [a] This is the planet that Pepe et al. (2007) and Santos et al. (2004) refer to as HD 160691 c.

with estimates for these systems varying by as much as 0.3 dex between different authors).

We also note that with a mass smaller than that of the Sun (0.85 $M_{\odot}$), the habitable zone for HD 102365 will lie at smaller orbital radii than it does for the Sun. For an Earth-like planet, Kasting et al. (1993) estimate the habitable zone for a 0.85 $M_{\odot}$ star to lie in the range 0.6–1.0 AU. Obviously, HD 102365 is *not* an Earth-like planet, and so such an estimate is not appropriate to the planet itself, which will have very different atmospheric properties to those assumed by Kasting et al. (1993). On the other hand, those assumptions *could* be valid for rocky satellites of HD 102365 b, if they exist. Unfortunately, HD 102365 b only approaches the inner edge of this habitable zone when it is near apastron for our eccentric orbital solution, and not at all for our circular orbital solution. So, HD 102365 b is a marginal target for "habitable" exomoons.

We acknowledge support from the following grants; NSF AST-9988087, NASA NAG5-12182, PPARC/STFC PP/C000552/1, ARC Discovery DP774000; and travel support from the Carnegie Institution of Washington and the Australian Astronomical Observatory (formerly the Anglo-Australian Observatory). We thank an anonymous referee for a rapid and helpful reading. We are extremely grateful for the extraordinary support we have received over the lifetime of the AAPS program from the AAT's technical staff: K. Fiegert, F. Freeman, S. James, G. Kitley, Y. Kondrat, S. Lee, R. Paterson, E. Penny, J. Pogson, G. Schaffer. D. Stafford, J. Stevenson, and T. Young. *Facilities:* AAT

REFERENCES

Bailey, J. A., Butler, R. P., Tinney, C. G., Jones, H. R. A., O'Toole, S. J., Carter, B. D., & Marcy, G. W. 2009, ApJ, 690, 743
Bond, J. C., Tinney, C. G., Butler, P. R., Jones, H. R. A., Marcy, G. W., Penny, A. J., & Carter, B. D. 2006, MNRAS, 370, 163
Bonfils, X., et al. 2005, A&A, 443, L15
Bonfils, X., et al. 2007, A&A, 474, 293
Bouchy, F., et al. 2009, A&A, 496, 527
Butler, R. P., Marcy, G. W., Williams, E., McCarthy, C., Dosanjh, P., & Vogt, S. S. 1996, PASP, 108, 500
Butler, R. P., Tinney, C. G., Marcy, G. W., Jones, H. R. A., Penny, A. J., & Apps, K. 2001, ApJ, 555, 410
Butler, R. P., et al. 2002, ApJ, 578, 565
Carter, B. D., et al. 2003, ApJ, 593, L43
Delfosse, X., Forveille, T., Ségransan, D., Beuzit, J.-L., Udry, S., Perrier, C., & Mayor, M. 2000, A&A, 364, 217
Diego, F., Charalambous, A., Fish, A. C., & Walker, D. D. 1990, Proc. SPIE, 1235, 562
Evans, D. S., Menzies, A., & Stoy, R. H. 1957, MNRAS, 117, 534
Fischer, D. A., et al. 2008, ApJ, 675, 790
Forveille, T., et al. 2009, A&A, 493, 645
Gray, R. O., et al. 2006, AJ, 132, 161
Hawley, S. L., Gizis, J. E., & Reid, I. N. 1996, AJ, 112, 2799
Hébrard, G., et al. 2010, A&A, 512, 46
Henry, T. J., Soderblom, D. R., Donahue, R. A., & Baliunas, S. L. 1996, AJ, 111, 439
Holmberg, J., Nordström, B., & Andersen, J. 2009, A&A, 501, 941

Howard, A. W., et al. 2009, ApJ, 696, 75
Howard, A., et al. 2010, ApJ, submitted (arXiv:1003.3444)
Ida, S., & Lin, D. N. C. 2004, ApJ, 604, 388
Ida, S., & Lin, D. N. C. 2005, ApJ, 626, 1045
Jones, H. R. A., Butler, R. P., Marcy, G. W., Tinney, C. G., Penny, A. J., McCarthy, C., & Carter, B. D. 2002, MNRAS, 333, 871
Jones, H. R. A., Butler, R. P., Marcy, G. W., Tinney, C. G., Penny, A. J., McCarthy, C., & Carter, B. D. 2003a, MNRAS, 337, 1170
Jones, H. R. A., Butler, R. P., Marcy, G. W., Tinney, C. G., Penny, A. J., McCarthy, C., Carter, B. D., & Pourbaix, D. 2003b, MNRAS, 341, 948
Jones, H. R. A., et al. 2006, MNRAS, 369, 249
Jones, H. R. A., et al. 2010, MNRAS, 403, 1703
Kasting, J. F., Whitmire, D. P., & Reynolds, R. T. 1993, Icarus, 101, 108
Keenan, P. C., & McNeil, R. C. 1989, ApJS, 71, 245
Laughlin, G., Bodenheimer, P., & Adams, F. C. 2004, ApJ, 612, L73
Laughlin, G., Butler, R. P., Fischer, D. A., Marcy, G. W., Vogt, S. S., & Wolf, A. S. 2005, ApJ, 622, 1182
Lo Curto, G., et al. 2010, A&A, 512, L48
Lomb, N. R. 1976, Ap&SS, 39, 447
Lovis, C., et al. 2006, Nature, 441, 305
Lovis, C., et al. 2010, A&A, submitted (arXiv:1011.4994)
Marcy, G. W., et al. 2005, ApJ, 619, 570
Mayor, M., et al. 2009a, A&A, 493, 639
Mayor, M., et al. 2009b, A&A, 507, 487
McArthur, B. E., et al. 2004, ApJ, 614, L81
McCarthy, C., et al. 2004, ApJ, 617, 575
Meschiari, S., Wolf, A. S., Rivera, E., Laughlin, G., Vogt, S., & Butler, P. 2009, PASP, 121, 1016
Mordasini, C., et al. 2010, A&A, in press (arXiv:1010.0856v1)
Noyes, R. W., Hartmann, L. W., Baliunas, S. L., Duncan, D. K., & Vaughan, A. H. 1984, ApJ, 279, 763
O'Toole, S., Tinney, C. G., & Jones, H. R. A. 2008, MNRAS, 386, 516
O'Toole, S., et al. 2007, ApJ, 660, 1636
O'Toole, S., et al. 2009, ApJ, 697, 1263
Pepe, F., et al. 2007, A&A, 462, 769
Perryman, M. A. C., et al. 1997, A&A, 323, L49
Rivera, E. J., Butler, R. P., Vogt, S. S., Laughlin, G., Henry, G. W., & Meschiari, S. 2010, ApJ, 708, 1492
Rivera, E. J., et al. 2005, ApJ, 634, 625
Santos, N. C., et al. 2004, A&A, 426, L19
Scargle, J. D. 1982, ApJ, 263, 835
Schröder, C., Reiners, A., & Schmitt, J. H. M. M. 2009, A&A, 493, 1099
Sousa, S. G., et al. 2008, A&A, 487, 373
Takeda, G., Ford, E. B., Sills, A., Rasio, F. A., Fischer, D. A., & Valenti, J. A. 2007, ApJS, 168, 297
Tinney, C. G., Butler, R. P., Marcy, G. W., Jones, H. R. A., Penny, A. J., McCarthy, C., & Carter, B. D. 2002, ApJ, 571, 528
Tinney, C. G., et al. 2001, ApJ, 551, 507
Tinney, C. G., et al. 2003, ApJ, 587, 423
Tinney, C. G., et al. 2005, ApJ, 623, 1171
Tinney, C. G., et al. 2006, ApJ, 647, 594
Udry, S., et al. 2006, A&A, 447, 361
Udry, S., et al. 2007, A&A, 469, L43
Valenti, J. A., Butler, R. P., & Marcy, G. W. 1995, PASP, 107, 966
Valenti, J. A., & Fischer, D. A. 2005, ApJS, 159, 141
Van Biesbrock, G. 1961, AJ, 66, 528
Vogt, S. S., Butler, R. P., Rivera, E. J., Haghighipour, N., Henry, G. W., & Williamson, M. H. 2010a, ApJ, 723, 954
Vogt, S. S., et al. 2005, ApJ, 632, 638
Vogt, S. S., et al. 2010b, ApJ, 708, 1366
Wittenmyer, R. A., Endl, M., Cochran, W. D., Hatzes, A. P., Walker, G. A. H., Yang, S. L. S., & Paulson, D. B. 2006, AJ, 132, 177
Wittenmyer, R. A., et al. 2010, ApJ, 722, 1854
Wright, J. T., Upadhyay, S., Marcy, G. W., Fischer, D. A., Ford, E. B., & Johnson, J. A. 2009, ApJ, 693, 1084